



## Strathprints Institutional Repository

**Tasca, Andrea Luca and Ghajeri, Farnaz and Fletcher, Ashleigh J. (2017) Novel hydrophilic and hydrophobic amorphous silica : characterization and adsorption of aqueous phase organic compounds. Adsorption Science & Technology. pp. 1-21. ISSN 2048-4038 (In Press) ,**

This version is available at <http://strathprints.strath.ac.uk/59437/>

**Strathprints** is designed to allow users to access the research output of the University of Strathclyde. Unless otherwise explicitly stated on the manuscript, Copyright © and Moral Rights for the papers on this site are retained by the individual authors and/or other copyright owners. Please check the manuscript for details of any other licences that may have been applied. You may not engage in further distribution of the material for any profitmaking activities or any commercial gain. You may freely distribute both the url (<http://strathprints.strath.ac.uk/>) and the content of this paper for research or private study, educational, or not-for-profit purposes without prior permission or charge.

Any correspondence concerning this service should be sent to Strathprints administrator: [strathprints@strath.ac.uk](mailto:strathprints@strath.ac.uk)

1 Novel hydrophilic and hydrophobic amorphous silica:  
2 characterization and adsorption of aqueous phase organic  
3 compounds

4 Andrea Luca Tasca,\*<sup>a</sup> Farnaz Ghajeri,<sup>b</sup> Ashleigh J. Fletcher<sup>a</sup>

5 <sup>a</sup> Department of Chemical and Process Engineering, University of Strathclyde, Glasgow G1  
6 1XJ, United Kingdom.

7 <sup>b</sup> Department of Engineering Sciences, Applied Materials Science, Uppsala University,  
8 Uppsala, Sweden

9 **Abstract**

10 Very few studies have investigated the adsorption performance of hydrophobic and  
11 hydrophilic silicas with dissolved organics in water, which is a required final step during  
12 produced water treatment. The cost of functionalization also hinders the use of hydrophobic  
13 materials as sorbents. Novel hydrophilic silicas, prepared at low temperature and ambient  
14 pressure, were characterised by SEM, FTIR and BET analysis, and studied for the adsorption  
15 of aqueous phase organic compounds at concentrations below their solubility limits.  
16 Adsorption capacities were found to be up to 264 mg/g for benzene and 78.8 mg/g for  
17 toluene. Direct comparison is made with the analogous hydrophobic version of one of the  
18 silica materials, demonstrating comparable uptakes for benzene concentrations lower than 50  
19 mg/L. This finding supports the hypothesis that, at very low aqueous phase organic  
20 concentrations, hydrophobicization has no discernible effect on access of the pollutants to the  
21 internal porosity of the material.

22 **Keywords**

23 Quartzene; benzene; toluene; produced water; GC

## 24 1. Introduction

25 Silica aerogels are materials with large surface areas, high porosities, low densities and  
26 conductivities, which can be successfully used as thermal insulators, catalyst supports,  
27 adsorbents, and in many other scientific and commercial applications (Wang et al., 2015).  
28 Researchers reported a  $\text{CF}_3(\text{CH}_2)_2$ - functionalized aerogel powder capable of absorbing up  
29 than 230 times its weight in oil (Reynolds et al., 2001), while further studies showed that  
30 such doped hydrophobic materials can adsorb more than 30 times the volume of toluene  
31 compared with Granular Activated Carbon (GAC) (Hrubesh et al., 2001). Silica gels,  
32 synthesised using tetramethoxysilane (TMOS) as the precursor, were modified by replacing  
33 the Si-OH groups, responsible for the adsorption of water, with S- $\text{CH}_3$  groups via addition of  
34 methyltrimethoxysilane (MTMS) and trimethylethoxysilane (TMES). Adsorption tests on the  
35 subsequent gels revealed maximum benzene adsorption capacities 300 times higher than  
36 GAC (Standeker et al., 2007), with equilibrium established in less than 30 min. Silica  
37 aerogels have been shown to uptake pure organic compounds, such as benzene and toluene,  
38 to levels in excess of 13 g/g aerogel (Wang et al., 2011). The high uptakes are mainly due to  
39 the resulting swelling of the adsorbent.

40 Consequently, aerogels have been studied extensively for the absorption of oil spills (Wang et  
41 al., 2012, Reynolds et al., 2001, Adebajo et al., 2003, Olalekan et al., 2014); however, despite  
42 their adsorption potential for organic species, they have not been used in water treatment  
43 plants for the separation of petroleum hydrocarbons. Several researchers have previously  
44 tested aerogels on crude oil-water mixtures, and it has been proven that functionalization with  
45 fluorinated organic groups, which maximises hydrophobicity, gives the best performance in  
46 terms of organic adsorption from pure oil or oil-water mixtures (Hrubesh et al., 2001, Wang  
47 et al., 2012).

48 An issue with these past studies is that many work at excessive concentrations of organic  
49 species within the aqueous phase; whereas produced water, at the refining stage, contains  
50 only low concentrations of dissolved oil droplets, mainly part of the BTEX group (benzene,  
51 toluene, ethylbenzene and xylene). Hence, it is essential to evaluate the adsorption  
52 performance of potential sorbent materials with concentrations of these pollutants well below  
53 the solubility limits. Previous work compared benzene adsorption isotherms, using aerogel  
54 materials, an activated carbon and a polymeric resin, at similar concentrations, and no free oil  
55 phase present in the batch tests; the results showed that greater amounts of benzene and  
56 toluene were adsorbed from aqueous solution using activated carbons or polymeric resins  
57 rather than functionalized aerogels (Wang et al., 2011). Using aqueous concentrations of  
58 selected organic pollutants at one tenth of their solubility limits, polymeric resin XAD4 and  
59 activated carbon AC F400 were shown to respectively adsorb 150 mg/g and 320 mg/g of  
60 benzene, 180 mg/g and 340 mg/g of toluene (Wang et al., 2011, Simpson et al., 1993).  
61 Hydrophobic silica aerogel 'Nanogel' TLD 301, the surface of which is decorated with  
62 trimethyl-silyl groups ( $-\text{Si}(\text{CH}_3)_3$ ), was recently tested for the adsorption of organic  
63 compounds from aqueous phase, using adsorbate concentrations below the water solubility  
64 limits. Equilibrium was reached in under 20 min and the adsorption capacities were 87 mg/g

65 for benzene and 223 mg/g for toluene, while the individual uptake of both organics, at  
66  $C = 0.1C_{SAT}$ , was found to be less than 10 mg/L (Wang et al., 2011). Recently aerogels  
67 obtained from methyltrimethoxysilane (MTMS) as a precursor and dried supercritically were  
68 shown to uptake more than 50 mg/g of benzene at a concentration of 50 mg/L of aqueous  
69 benzene, which is a significant result at such a low concentration (Perdigoto et al., 2012).

70 The results discussed above suggest that hydrophobic silica aerogels could be potential  
71 adsorbents for the treatment of oil spills. Hence, previous research has focussed markedly on  
72 hydrophobic media, with no known studies specifically related to the uptake of aqueous  
73 phase BTEX organics using hydrophilic silicas; consequently, many studies have focussed on  
74 improving the hydrophobicity of these materials. Hydrophobization of the inner surfaces of  
75 aerogels not only improves affinity to organic adsorbates, but it also helps to prevent long-  
76 term deterioration of the structure, due to the absorption of water; if water fills the pores of an  
77 aerogel and subsequently evaporates, then this acts as a second drying cycle and the structure  
78 can collapse, at least partially (A. Venkateswara Rao and A. Parvathy Rao, 2011). The need  
79 to recycle hydrophilic silicas may be considered irrelevant if the absence of functionalising  
80 agents and the use of cheaper precursors and synthesis make the production and waste  
81 management of these materials economically suitable for a single adsorption cycle, hence,  
82 removing regeneration costs and associated issues. Such gains may be achieved by using  
83 simpler, less energy intensive processing methods and low cost synthetic routes using  
84 ambient pressure drying are already known to produce silica aerogels, from waterglass, with  
85 excellent mechanical properties (Zong et al., 2015).

86 In this paper, we propose a study of hydrophilic silicas that have been seemingly overlooked  
87 for organics removal from aqueous systems in the past. Hence, we characterise both  
88 hydrophilic and hydrophobic amorphous silicas, determining and comparing their kinetics  
89 and capacities of adsorption to selected organic species from aqueous media at a range of  
90 different concentrations below the solubility limit. Thus, allowing evaluation of the  
91 feasibility of the use of these materials as sorbents for produced water treatment.

## 92 **2 Experimental**

### 93 **2.1 Adsorbents**

94 Four Quartzene based sorbents were used in the study, namely: ND, Z1, Z1HPO and CMS  
95 types, all supplied by Svenska Aerogel AB (SvAAB). The structure of Quartzene and its  
96 properties are comparable to silica aerogels but the former is an amorphous silica material.  
97 Both have skeletal structures composed of porous silica, very low densities, and very low  
98 thermal conductivities. The only significant physical difference is that Quartzene is produced  
99 as a powder, not as a gel from a sol-gel process. Its chemical properties, in terms of  
100 hydrophilicity/hydrophobicity, can be tailored to fit a specific application and the porous  
101 structure can also be controlled, notably without the need of a surfactant. Unlike traditional  
102 aerogels, Quartzene is an environmentally friendly material, which is significantly cheaper to

103 produce, as a result of the ambient pressure and temperature conditions used in its  
104 manufacture.

105 **ND type Quartzene:** prepared via the precipitation of sodium silicate with sodium chloride  
106 at ambient temperature. A defined amount of dilute active aqueous sodium silicate solution  
107 ( $\text{SiO}_2:\text{Na}_2\text{O} = 3.35$ ) was prepared, representing solution A, while solution B was composed  
108 of aqueous sodium chloride (NaCl). Solutions A and B were mixed under rapid stirring and  
109 the resulting precipitate mixed with a defined amount of tap water, before vacuum filtration  
110 through a filter paper until a paste, comprising up to 85% water, was obtained and dried via  
111 spray drying. **Z1 type Quartzene samples:** prepared using a method analogous to that for  
112 ND but with a different level of activation of the silica source (Twumasi Afriyie et al., 2014).  
113 Furthermore, a methylated version of Z1, herein called Z1HPO, was developed by Svenska  
114 Aerogel AB, allowing direct comparison of adsorption uptakes and kinetics between  
115 hydrophilic and hydrophobic versions of the same base material. **CMS type Quartzene:**  
116 prepared by adding calcium and magnesium sources at concentrations of 1:2 to the silica  
117 source (Waterglass  $\text{SiO}_2/\text{Na}_2\text{O} = 3.35$ ). A 500 ml salt solution, consisting of  $\text{MgCl}_2$   
118 hexahydrate and  $\text{CaCl}_2$  dihydrate was prepared at a ratio of 68 mol% Mg and 32 mol% Ca;  
119 500 ml salt solution, was poured onto 1.5 M (with respect to  $\text{SiO}_2$ ) sodium silicate solution  
120 (500 ml), and the resulting mixture agitated at room temperature. Subsequent coagulation  
121 occurred, as previously described (Twumasi Afriyie et al., 2013), and the obtained gel was  
122 washed, filtered and dried in the same manner as ND.

123 ND and CMS type samples used in this study were powders, with particle sizes between 2  
124 and 150  $\mu\text{m}$ , and  $D_{v90}$  (particle size below which 90% of the sample falls) equal,  
125 respectively, to 46 and 75  $\mu\text{m}$ , measured with a Malvern Hydro 2000S. Granules of Z1 and  
126 Z1HPO were also used, with particle sizes between 1 and 1.5 mm.

### 127 **2.1.1 Characterization of adsorbents**

128 Samples were dried for 2 h at 358 K prior to coating with a thin layer (1.5 nm) of gold for  
129 FE- SEM analysis using a HITACHI SU-6600 (2010) Field Emission Scanning Electron  
130 Microscope. The instrument is equipped with Energy Dispersive Spectroscopy (EDS),  
131 Oxford Inca 350 with 20mm X-Max detector and Wavelength Dispersive Spectroscopy  
132 (WDS), and uses Oxford Inca Wave 700 Microanalysis System with Energy + Software.

133 Surface chemical functionalities of adsorbent materials are known to determine their  
134 hydrophilic or hydrophobic nature and this is also true of silicas (El Rassy and Pierre, 2005).  
135 FT-IR analysis, obtained using an ABB MB 3000 spectrophotometer with Horizon MB™  
136 FTIR software, were used to determine surface functionalities of samples (dried at 248 K for  
137 2 h) prepared as hydrophilic.

138 Nitrogen sorption measurements were performed at 77 K using a Micromeritics ASAP 2420,  
139 on samples accurately weighed between 0.15 and 0.5 g and degassed at 393 K, for 3.5 h.  
140 Degassing at low temperatures requires longer treatment times but has the benefit that the

141 structure of the material is preserved. Forty adsorption points and thirty desorption points  
142 were collected per isotherm, spanning the relative pressure range 0 - 0.99. BET analysis  
143 (Brunauer et al., 1938) was used to interpret the data obtained.

144 A film of adsorbate is known to cover an adsorbent with a defined density profile but, by  
145 assuming that the film thickness is uniform, it is possible to obtain a ‘statistical thickness’ (t)  
146 from gas sorption isotherms, such as the nitrogen sorption analysis used here. The Harkins-  
147 Jura thickness equation, derived from Lippens and De Boer’s analysis for non-porous  
148 siliceous materials characterised by nitrogen adsorption at 77 K (Lippens and De Boer,  
149 1965), can be employed as a reference, to estimate surface area, average pore size and pore  
150 volume of materials with similar composition and BET C constants, using the t-plot analysis  
151 method. An assumption of the t-plot method is the uniformity of the thickness of the  
152 adsorbent layer, hence, adsorption on a mesoporous surface is considered similar to  
153 adsorption on a flat surface; however, the adsorbed thickness on small mesopores is not  
154 constant, but varies as a function of the pore diameter. Consequently, this method, when  
155 applied to nitrogen adsorption, should be used with caution in the presence of mesopores with  
156 diameters < 3.5 nm (Galarneau et al., 2014), which, in this study, includes ND samples.  
157 Furthermore, it is essential that the reference surface should be energetically and structurally  
158 similar to the porous solid surface under analysis, as both factors affect the level of adsorbate  
159 loading at a given relative pressure; however, the BET C value does not guarantee a similar  
160 surface structure, so it is not sufficient basis for selection of a reference isotherm (Biggs et  
161 al., 2004). For these reasons, surface areas and pore volumes reported in this study were  
162 estimated using  $\alpha$ -plot analysis, as this is considered more reliable than the t-plot method.

163 Parameters of the reference adsorbent Lichrospher-1000 were applied in the following  
164 equation (Gregg and Sing, 1982):

$$165 \quad a(x) = a + k_{st} S_{ext} \alpha_s(p/p_0)$$

166 Where: a is the intercept with the y-axis, related to the adsorption in saturated micropores;  $k_{st}$   
167 =  $a_{st}(x = 0.4) / S_{st}$ , where  $S_{st}$  is the specific surface area of the reference material;  $\alpha_s$  =  
168  $a_{st}(p/p_0) / a_{st}(p/p_0 = 0.4)$ ; and  $S_{ext}$  = external surface area of the adsorbent analysed.

## 169 **2.2 Adsorptives**

170 Benzene and toluene were used in this study as representative components of dissolved oils in  
171 produced water from the BTEX family; the organics were purchased from Sigma Aldrich as  
172 chromatography grade reagents (HPLC,  $\geq 99.9\%$ ). Benzene is more representative of  
173 dissolved oil, as the most difficult of the BTEX group to adsorb from solution, due to the fact  
174 that the adsorption potential of the solute in the liquid carrier decreases with increasing  
175 solubility of the adsorbate. Since, the solubility of the monoaromatics in the BTEX group  
176 decreases with molecular weight, their adsorption potential increases with the molecular

177 weight (Wang et al., 2011), hence, the lowest molecular weight species (benzene) is the most  
178 difficult to adsorb.

### 179 **2.3 Adsorption experiments**

180 Borosilicate glass bottles were used for all adsorption studies, and bottle volumes were  
181 selected in order to reduce headspace within the vessel. Mixtures of water and benzene were  
182 stirred in filled bottles for 1 h using a magnetic stirrer to solubilize the organic, before  
183 samples were extracted with a micropipette, then mixed with methanol and internal standard  
184 before injection, using a microsyringe, into the port of a Shimadzu GC 2014 gas  
185 chromatograph equipped with FID detectors to determine the concentration present. Pre-  
186 determined amounts of adsorbent were added to prepared bottles of aqueous phase organics  
187 to study adsorption characteristics. Kinetic tests were conducted at pre-determined intervals,  
188 over 24 h, to determine times for maximum equilibria to be achieved for each sample; the  
189 aqueous concentrations of benzene and toluene were respectively ~1 g/l and ~0.35 g/L. All  
190 measurements were conducted at 293 K.

191 Adsorption tests involved the addition of benzene, at concentrations in the range 0 -  
192 1100 ppm, to 110 ml of distilled water mixed with 100 - 500 mg of adsorbent, equilibrated  
193 for 24 h before analysis. An analogous procedure was used for toluene but using aqueous  
194 concentrations in the range 0 - 400 ppm.

195 The adsorption behaviour of hydrophobic Z1HPO was only tested using aqueous benzene,  
196 agitated using a rotary shaker to guarantee sorbent contact with the aqueous phase, which  
197 could not be guaranteed by use of a magnetic stirrer, as used for the hydrophilic materials,  
198 due to the fact that the light hydrophobic material floats in water. All procedures were  
199 performed at 293 K using sealed cups with minimal headspace, as outlined above, to reduce  
200 volatilisation losses. Lower temperatures were not investigated as the reduction in  
201 temperature significantly impacts on kinetic performance by increasing the time required for  
202 equilibration and making kinetic measurements impractical. Blank tests, conducted without  
203 sorbent, demonstrated that volatilisation rates were negligible for both kinetic and adsorption  
204 measurements. The stirring rates used were constant, at 200 rpm for magnetic stirring and 20  
205 rpm for rotary stirring. Sampling was performed at various depths within a selected test  
206 vessel to verify the absence of concentration gradients within the bulk.

### 207 **2.4 Measurement of organic concentrations: gas chromatography**

208 Gas chromatography, using a Shimadzu GC 2014 gas chromatograph equipped with FID  
209 detectors was used to measure the concentrations of organic species in the aqueous systems  
210 studied. A fused silica chromatographic capillary column (5% diphenyl/95% dimethyl  
211 siloxane phase), 25 m x 0.32 mm, was used. The column was purchased from Sigma Aldrich  
212 and conditioned at 553 K for 3 h before first use. Samples were extracted and placed in sealed  
213 vials, to which the solvent (methanol) and internal standard were also added; from these vials,  
214 1  $\mu$ L was removed, by microsyringe, and injected into the chromatograph sample port,

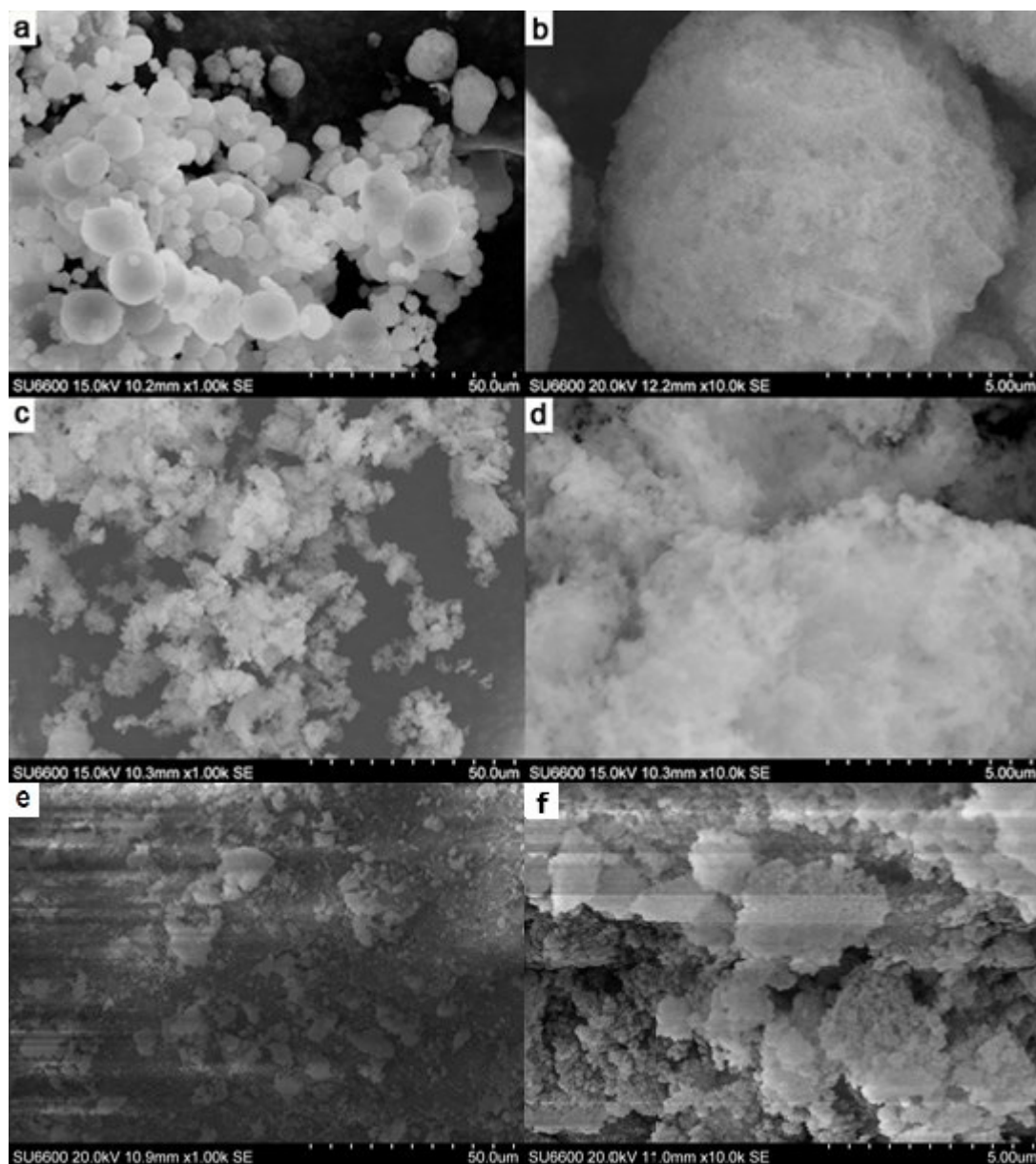
215 piercing a rubber septum. Toluene was used as the internal standard for benzene, and vice  
216 versa; the construction of a calibration curve allowed direct comparison of peak ratios, thus,  
217 the determination of the concentration of the organic species in the test system. Column  
218 flows, oven and detector temperatures were evaluated to optimise peak resolution; parameters  
219 used in this study were: carrier gas: helium; injection: splitless; injector temperature: 523 K;  
220 detector temperature: 523 K; column flow: 1.5 ml/min; purge flow: 2.5 ml/min; oven  
221 program: 4 min at 323 K, ramp to 453 K at 10 K/min, ramp to 673 K at 10 K/min ,with final  
222 holding time of 5 min. Analyses were run in duplicate to ensure equipment precision;  
223 additional experiments were conducted on different days, both within a continuous series of  
224 analyses, and once on cold start-up, to verify reproducibility of results.

## 225 **3 Result and Discussion**

### 226 **3.1 Characterization results**

227 The results of FE-SEM analysis are presented in Figure 1 and it is evident that the observed  
228 networks are quite different despite the similarity of their synthetic processes.



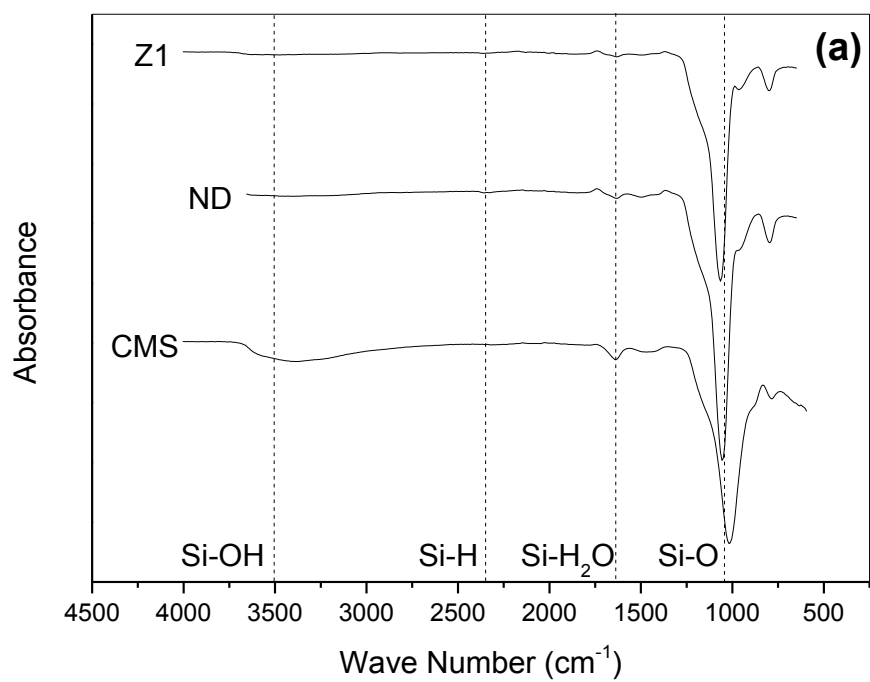


229

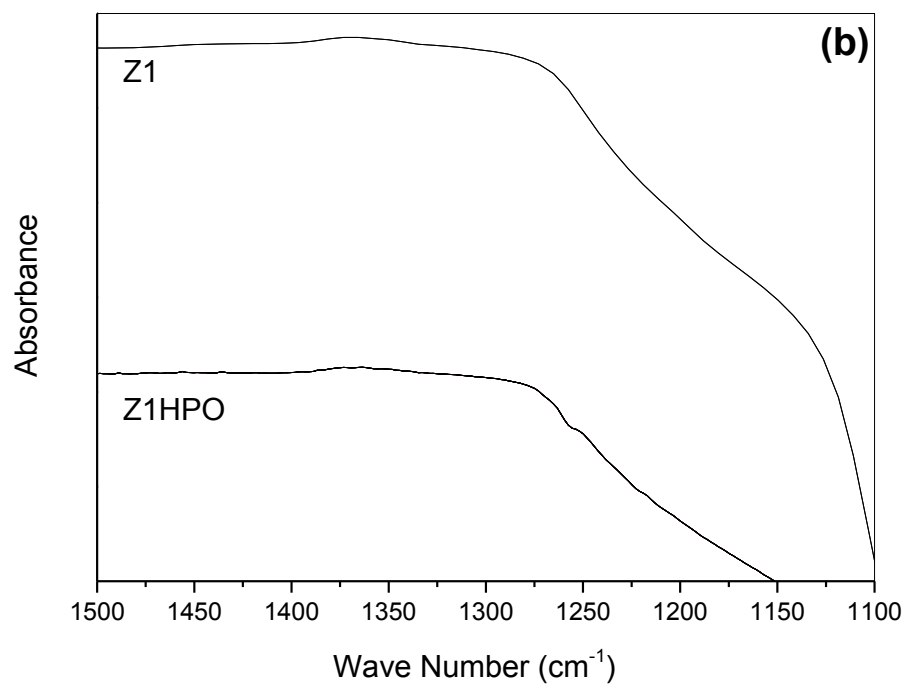
230 **Figure 1:** FE-SEM analysis of Quartzene samples: CMS (a: x1k, b: x10k), ND (c: x1k, d: x  
 231 10k) and Z1 (c: x1k, d: x 10k).

232 The obtained FTIR spectra (Figure 2) show the presence of silanol polar groups (Si-OH), in  
 233 the range  $2700 - 3650 \text{ cm}^{-1}$ , for all materials studied, with Z1 and ND showing similar surface  
 234 chemistries, while CMS exhibits more refined Si-OH bond peaks; consequently, these  
 235 Quartzene materials can be categorised as hydrophilic in nature. The FTIR spectra of Z1HPO  
 236 shows a small peak around  $1250 \text{ cm}^{-1}$ , attributed to the Si-CH<sub>3</sub> bonds, formed as consequence  
 237 of the functionalization process. The presence of CO<sub>2</sub> can produce an absorption peak at  
 238  $\sim 2300 \text{ cm}^{-1}$ , however, immediately prior background measurements were used to account for  
 239 its atmospheric presence and as the peak observed for Si-H occurs for all samples, this  
 240 provides evidence of such functionality in the materials used.

241



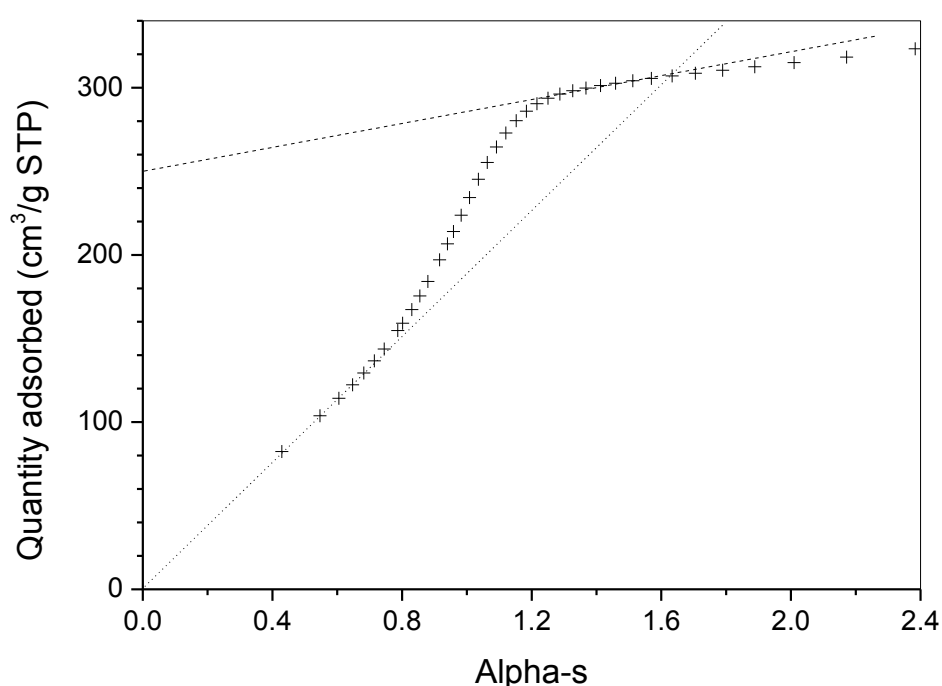
242



243

244 **Figure 2:** FT-IR spectra of silica samples: (a) Z1, ND and CMS and (b) comparison between  
245 the FT-IR spectra of Z1 and hydrophobic Z1HPO. The presence of Si-CH<sub>3</sub> bonds in the  
246 sample Z1HPO is confirmed by the small peak around 1250 cm<sup>-1</sup>.

247 Figure 3 shows the  $\alpha$ -plot analysis of the nitrogen adsorption isotherm obtained at 77 K for  
248 Quartzene ND. The gradient of the solid line provides an estimation of the total specific  
249 surface area, while the gradient of the upper dashed line corresponds to the surface area  
250 external to the primary mesopores, which is ascribed as the surface area of any large  
251 mesopores and macropores present in the material. The intercept of the dashed line provides  
252 an evaluation of the already filled small mesopores, i.e. the small mesopore volume.



253

254 **Figure 3:**  $\alpha$ -plot analysis of ND nitrogen adsorption isotherm measured at 77 K (dotted line  
255 fit of low pressure data, dashed line fit of high pressure data).

256 The surface areas obtained for the four samples studied here show good agreement between  
257 the two methods (BET and  $\alpha_s$ ), except in the case of ND, which exhibits small mesopores  
258 (Table 1), thereby suggesting the value obtained using the  $\alpha$ -plot method would be more  
259 accurate. Pore sizes determined for CMS, Z1 and Z1HPO samples are widely distributed  
260 between 2 and 80 nm, while ND exhibits a discrete pore size distribution centred around  
261 3.3 nm (Table 1). Consequently, ND is the only materials with a small mesopore contribution  
262 but it is notable that all samples exhibit significant total pore volume.

263 **Table 1:** Surface areas and porosities of samples used in this study.

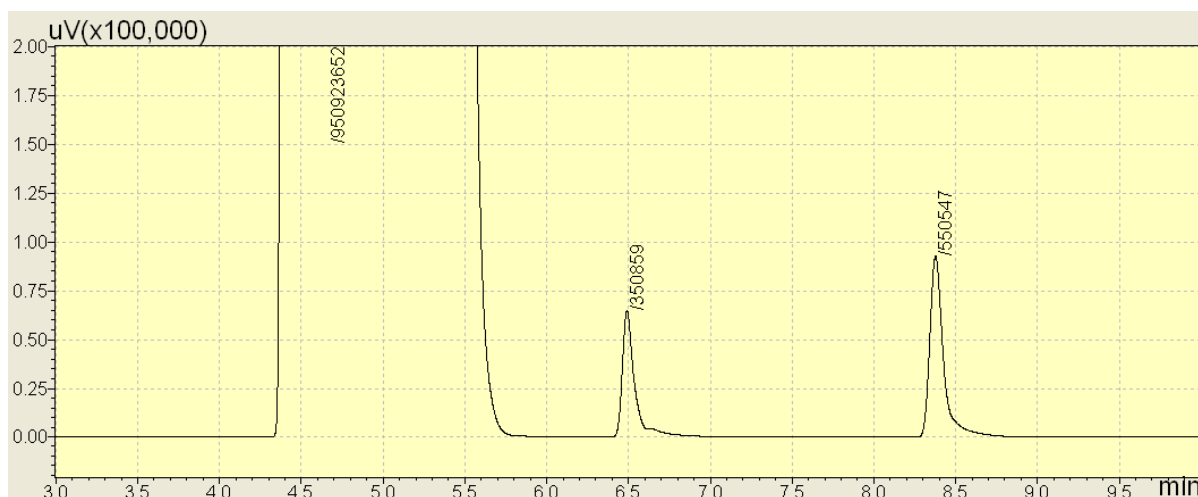
Sample name	Z1	Z1HPO	CMS	ND <sup>§</sup>
S <sub>BET</sub> / m <sup>2</sup> g <sup>-1</sup> †	325	186	158	597
S <sub>as</sub> / m <sup>2</sup> g <sup>-1</sup>	331	186	161	546
Average pore width / nm	20.3	17.4	14.6	3.3
Total pore volume / cm <sup>3</sup> g <sup>-1</sup>	1.03	0.97	0.50	0.54
Small mesopore volume / cm <sup>3</sup> g <sup>-1</sup> ‡	-	-	-	0.40
Meso and macro-pore volume / cm <sup>3</sup> g <sup>-1</sup> ‡	1.03	0.97	0.50	0.14

264 † BET linearization ( $p/[n_a \cdot (p^\circ - p)]$  vs.  $p/p^\circ$ ) was performed over the relative pressure range 0.05-0.3.

265 ‡ Pore volume contributions were determined using the  $\alpha_s$  method.

266 §  $\alpha$ -plot for ND exhibits two ranges of mesoporosity (Figure 3); surface area of small mesopores is estimated as  
267 524 m<sup>2</sup>/g.

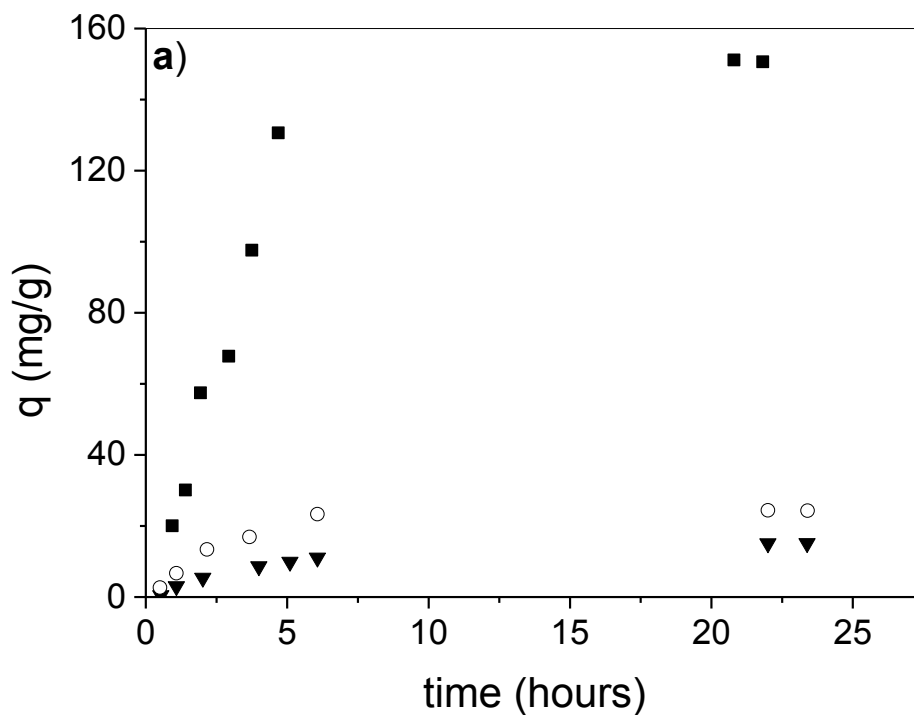
268 The low flow used for the carrier gas in the chromatography analyses was imperative to allow  
269 separation of the solvent and benzene peaks (Figure 4). The larger peak, beginning at  
270 4.3 min, is due to the solvent (methanol), followed by the benzene peak (elution time: 6.5  
271 min) and finally the toluene peak (elution time: 8.3 min).



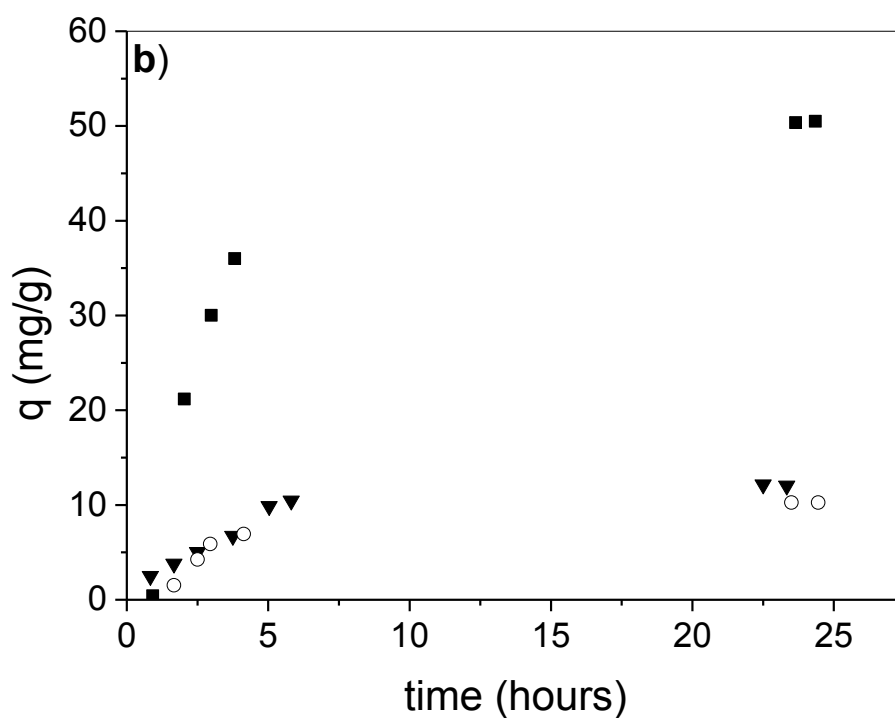
272  
273  
274 **Figure. 4:** Gas chromatograph analysis of aqueous benzene, with toluene as internal standard  
275 and methanol as solvent. x-axis: time/min; y axis: signal/ $\mu\text{V} \cdot k$ , where k is the magnification  
276 factor.

277 **3.2 Kinetic analysis and isotherms of the hydrophilic materials**

278 Kinetic data were obtained as outlined above and the results show a logarithmic relationship  
279 for the first 6 h of data, in which 84-90% of adsorption take place on CMS and NDsamples  
280 (Figure 5). The full equilibration time is less than 24 h, for both benzene and toluene uptake.



281



282

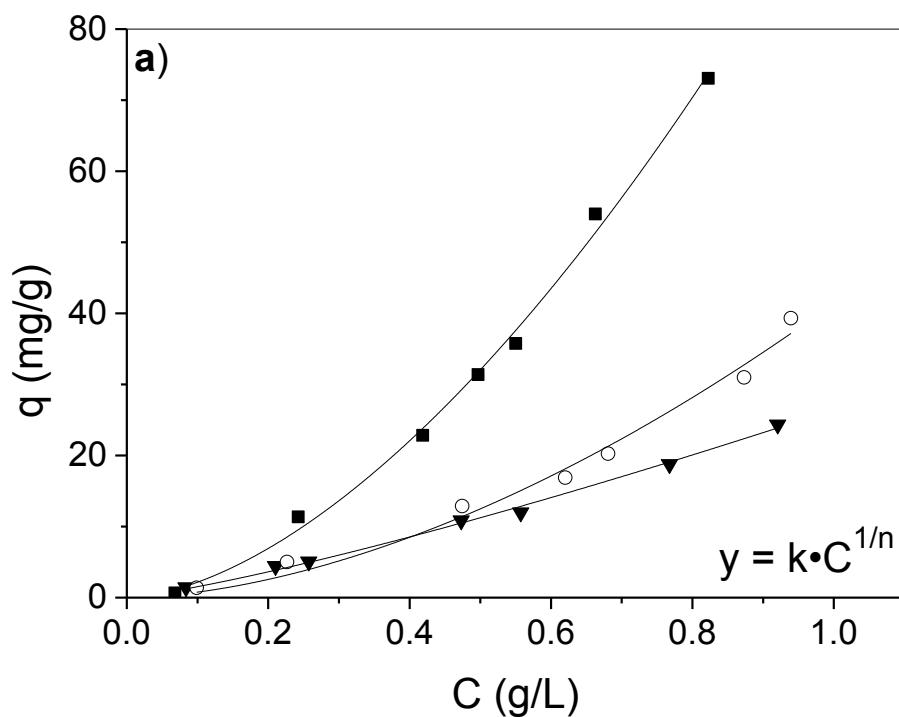
283 **Figure 5:** Kinetic profiles of (a) benzene and (b) toluene adsorption on Z1 (filled triangle),  
284 ND (filled square) and CMS (empty circle) at 293 K.

285 Quartzene Z1 shows slower kinetics, with < 80% of toluene and < 70% of benzene adsorbed  
286 after 24 h. Hydrophobic silica aerogels have been shown to reach their full adsorption  
287 capacities in < 1 h (Perdigoto et al., 2012) or even < 30 min (Standeker et al., 2007), the  
288 materials tested here show good short time performance but it should be noted that full  
289 equilibration takes several hours.

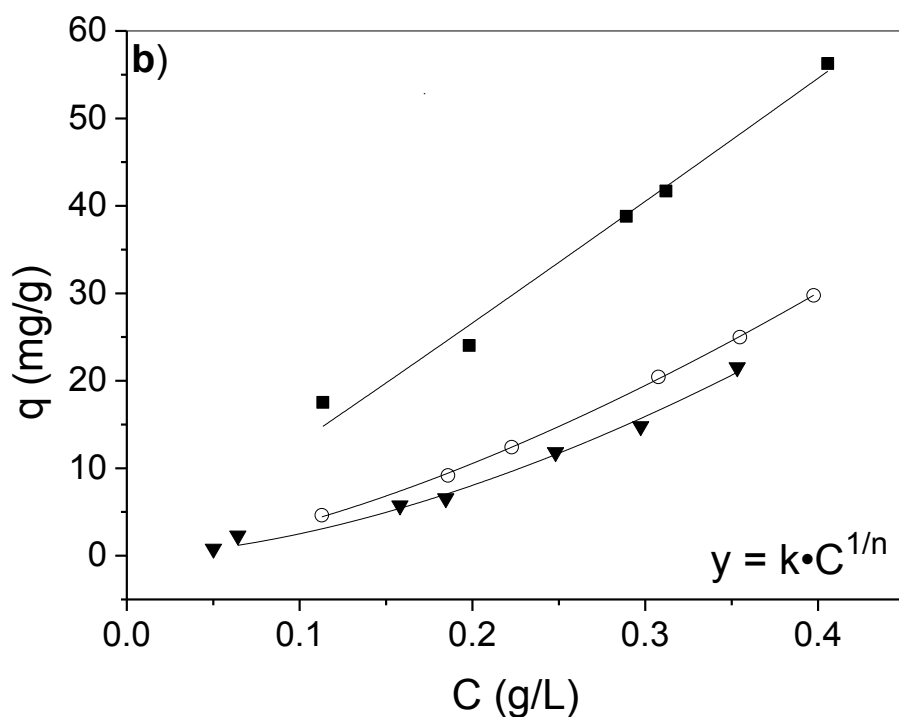
290 The Freundlich adsorption model (Freundlich and Hatfield, 1926) has been used extensively  
291 to determine adsorption capacities, mainly due to the fact that it considers the heterogeneity  
292 of real surfaces:

$$293 \qquad \qquad \qquad \mathbf{q = k \cdot C_e^{1/n}} \qquad \qquad \qquad \mathbf{(1)}$$

294 Where  $q$  is equilibrium uptake (mg adsorbate/g adsorbent);  $C_e$  is the equilibrium  
295 concentration of the solute (mg/L);  $k$  is the unitless constant of adsorption, indicating  
296 capacity;  $1/n$  is a unitless constant related to the intensity of adsorption. Higher values of  $k$   
297 indicate higher maximum adsorption capacity; while higher  $1/n$  values ( $> 1$ ) denote  
298 unfavourable adsorption. The  $1/n$  values obtained in this study are all more than unity, hence,  
299 adsorption for all materials with both adsorbates is dominated by physical sorption, as  
300 opposed to chemical sorption (Jiang et al., 2002).



301



302

303 **Figure 6:** Adsorption isotherms for benzene (a) and toluene (b) on Z1 (filled triangles), ND  
 304 (filled squares) and CMS (empty circles) at 293 K.

305 Aerogels studied previously show higher uptakes for toluene compared to benzene, however,  
 306 it is important to note that such results are based on adsorption isotherms obtained for two

307 adsorptives with disparate solubility limits; consideration of the parameters obtained by  
308 Freundlich analysis show that, while  $k$  values support this observation, the  $1/n$  values  
309 demonstrate the theoretical maxima would be greater for benzene, in agreement with  
310 previous findings (Standeker et al., 2007, Wang et al., 2011). Such high concentration  
311 behaviour is observed as a possible consequence of the delocalisation of the ring in benzene,  
312 which is reduced for toluene; also the functional group of toluene may cause associated  
313 packing effects, reducing the effective adsorption capacity, hence the maximum adsorption  
314 uptake, but only at high theoretical maximum concentrations. It can be seen, from Table 4,  
315 that the ND and CMS samples perform best from the three sorbents studied in the range of  
316 concentrations used, as supported by the  $k$  values obtained from Freundlich analysis, with  
317 maximum adsorption capacities for ND estimated as close to the adsorbate solubility limits:  
318 78.8 mg/g and 264 mg/g for toluene and benzene, respectively. The higher adsorption of  
319 Quartzene ND is ascribed, not only to the comparatively high surface area of this material but  
320 also, to its discrete pore size distribution centred around 3.3 nm, which provides good access  
321 for the organic molecules of interest while also being sufficiently narrow to prevent the  
322 molecular repulsion that can be observed with large adsorbate clusters. The results obtained  
323 for Z1 show a greater  $1/n$  value for toluene compared to benzene, which is contrary to  
324 previous findings and the other data reported here. Z1, which was the only original material  
325 used in granular form, underwent significant mechanical degradation during stirred reaction  
326 experiments. Z1 is produced with a different level of activation of the silica source with  
327 respect to ND, resulting in low surface area, porosity, and subsequent adsorption capacity.  
328 While mechanical degradation, due to the stirring procedure, is expected to occur also for the  
329 granular forms of ND and CMS (here tested as powders), the lower adsorption of Z1, which  
330 is also lower than for CMS, is likely due to the collapse of the pore structure of Z1 after  
331 immersion in water. Indeed, the level of activation of the silica source is expected to  
332 influence the silica xerogel and aerogel network strength.

333 **Table 2:** Freundlich adsorption model parameters calculated using data obtained for  
334 adsorption of toluene and benzene of samples used in this study, measured at 293 K.  
335 Maximum uptakes are determined from extrapolative interpolation to either a benzene  
336 solubility of 1.763 g/L or a toluene solubility of 0.57 g/L (Stephen and Stephen, 1963).

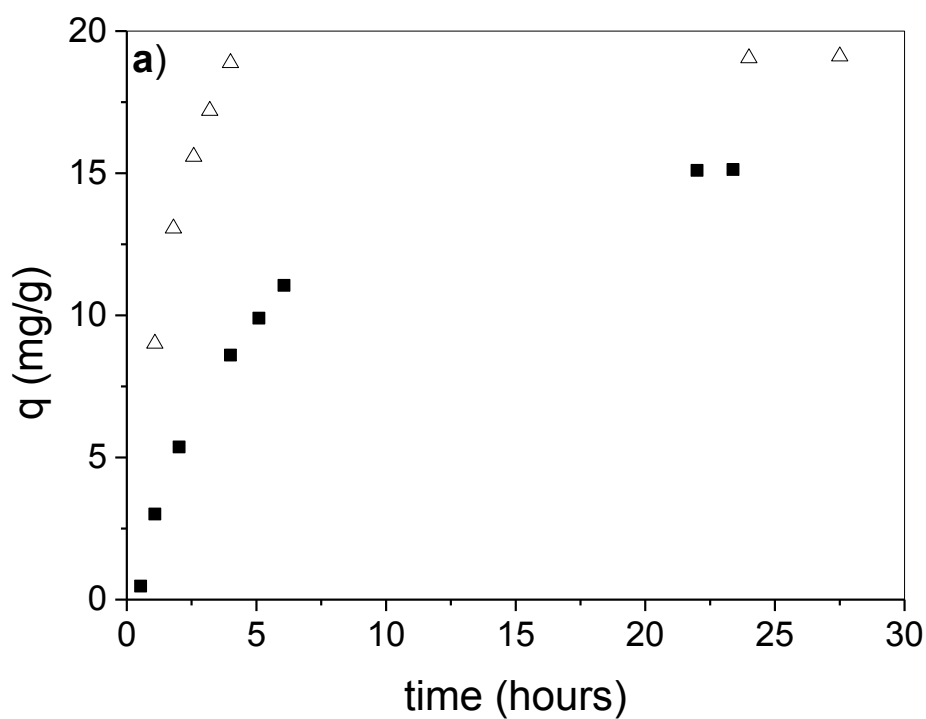
Adsorbate	Sample	K	1/n	Adj. R <sup>2</sup>	Max uptake / mg g <sup>-1</sup>
benzene	Z1	26.44	1.23	0.9954	53.25
	ND	102.23	1.67	0.9950	264.03
	CMS	41.42	1.73	0.9820	110.48
toluene	Z1	120.81	1.68	0.9861	46.91



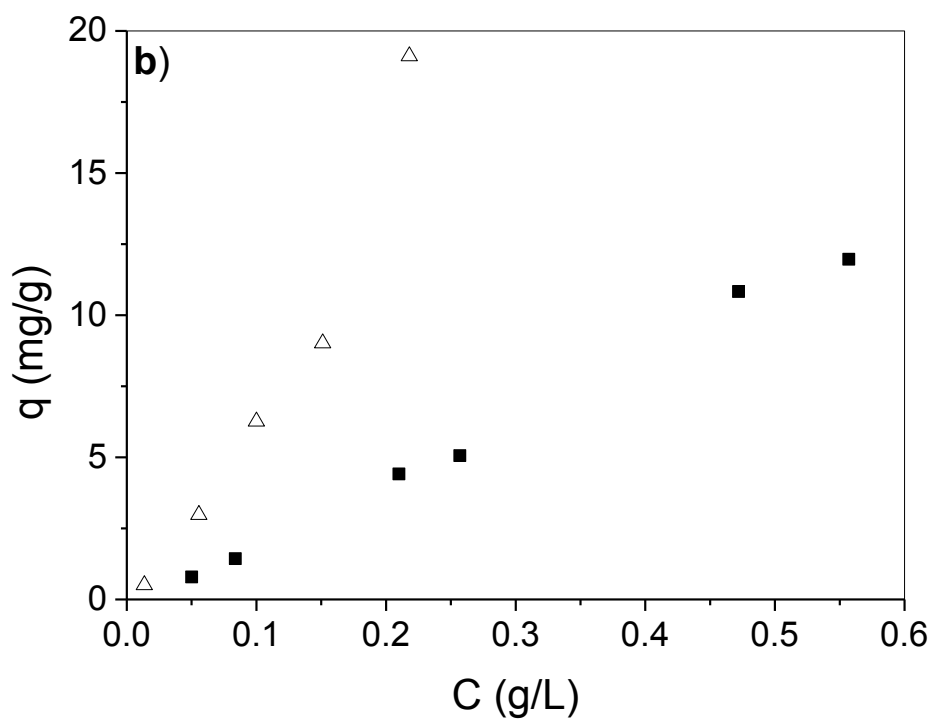
	ND	141.15	1.04	0.9890	78.82
	CMS	120.09	1.51	0.9995	51.36

337 **3.3 Comparison of hydrophilic and hydrophobic version of Z1**

338 Only aqueous benzene concentrations below 0.25 ppm were explored in the comparison of  
339 adsorption characteristics the hydrophilic and hydrophobic versions of Z1. Adsorption was  
340 faster and a higher quantity of benzene was adsorbed for Z1HPO (Figure 7); furthermore, this  
341 material showed no significant mechanical degradation even after five days of rotary stirring  
342 at 20 rpm.



343



344

345 **Figure 7:** Kinetics (a) and isotherms (b) obtained for benzene adsorption by granular forms  
 346 of Quartzene Z1 (filled squares) and Z1HPO (empty triangles) at 293 K.

347 Equilibrium was reached in less than 3 h for Z1HPO, while previously studied hydrophobic  
 348 aerogels, particle size < 250  $\mu\text{m}$ , were found to reach full adsorption capacity in less than 1 h,

349 adopting a similar method and rate of stirring (Perdigoto et al., 2012); this difference is likely  
350 due to differences in particle size, with a much larger particle size studied here. Testing the  
351 granular form of sorbents, as opposed to powders, provides greater insight in to material  
352 performance within a filter configuration, which is the most probable layout in a tertiary  
353 process dedicated to organics separation from water. The comparison of adsorption behaviour  
354 for hydrophilic Z1 and hydrophobic Z1HPO confirms that hydrophobicization is fundamental  
355 to multiple cycle use of a material. At high benzene concentrations, adsorption on Z1HPO is  
356 significantly higher than for Z1, but the difference in terms of uptake between the two  
357 adsorbents is reduced with decreasing organic concentration. Hence, at very low aqueous  
358 concentrations of organics, the effect of hydrophobicization on pollutant access to the internal  
359 porosity of the material may be not great enough to justify the expense of the  
360 functionalization process. Recently, it was proposed that organics dissolved in aqueous media  
361 in very diluted systems are unable to access the interior porosity of functionalized silica  
362 aerogels as a consequence of their inherent hydrophobic nature, suggesting that only the  
363 external surfaces are available for adsorption (Shi et al., 2014). These findings suggests a  
364 necessity to test adsorption performances of both hydrophilic and hydrophobic materials,  
365 especially when target organic pollutant concentrations are low enough as to make the  
366 economic profit of cyclic use, and associated regeneration costs, questionable given the  
367 expense of sorbent functionalization.

## 368 **4 Conclusions**

369 Novel hydrophilic amorphous silicas were synthesized at low temperature and ambient  
370 pressure. Two samples with varied levels of silica source activation, and one sample prepared  
371 via the addition of calcium and magnesium sources (ratio of 1:2) were tested for the  
372 adsorption of aqueous phase organics (benzene and toluene), at concentrations below their  
373 solubility limits. Kinetic tests reveal up to 90% of benzene and toluene is adsorbed in the  
374 first 6 h of treatment, and up to 50% in the first 2 h. There are no significant differences  
375 between the rates of adsorption for either benzene or toluene. The adsorption mechanism is  
376 favourable and described fully by the Freundlich model, with  $1/n > 1$  and higher for both  
377 adsorbates, while the adsorption capacity, at low concentrations, is higher for toluene, as  
378 expected from the literature (Love et al., 2003, Standeker et al., 2007).

379 Quartzene ND outperforms the other materials tests and shows adsorption capacities of 264  
380 mg/g for benzene (solution concentration of 1.76 g/L) and 78 mg/g for toluene (solution  
381 concentration of 0.57 g/L). By testing materials in a granular, the results provided a clearer  
382 indication of how the material can be expected to perform in a filter configuration, which is  
383 the most likely tertiary treatment process layout for organics separation from water. The  
384 comparison between hydrophilic Z1 and hydrophobic Z1HPO demonstrated that  
385 hydrophobicization is required to impart the mechanical longevity required for cyclic use,  
386 and leads to increased adsorption of benzene from aqueous phase concentrations  $> 50$  ppm. It  
387 is notable that the observed differences in uptake between the two forms of Z1 are reduced as  
388 organic concentration decreases. This finding supports the hypothesis that, at very low

389 aqueous phase organic concentrations, the effect of hydrophobicization on access of the  
390 pollutants to the internal porosity of the material may be not great enough to justify the  
391 expense of the functionalization process. Hence, tuning the hydrophobicity of sorbents to  
392 perform multiple adsorption cycles, with the added costs of regeneration should be fully  
393 evaluated via a cost analysis to determine whether the actual pollutant concentrations are  
394 significantly high to justify the expense of a functionalization process.

395 The adsorption results presented in this paper suggest that amorphous silica, such as  
396 Quartzene based materials, are a promising family of sorbent materials for application in the  
397 final stages of produced water treatment. To establish their full capabilities, defined ranges of  
398 pollutant concentration should be identified to allow selection of the most appropriate  
399 hydrophilic or hydrophobic material type, with additional lifetime cycling measurements to  
400 assess the economic feasibility of their use in water treatments plants.

## 401 **Acknowledgements**

402 The authors kindly thank Svenska Aerogel AB for providing adsorbent materials and  
403 associated particle size distribution data.

## 404 **References**

- 405 A. VENKATESWARA RAO, G. M. P., UZMA K. H. BANGI, & A. PARVATHY RAO, A.  
406 M. M. K. 2011. Sodium Silicate Based Aerogels via Ambient Pressure Drying  
407 *In: AEGERTER, M. A., LEVENTIS, N. K., MATTHIAS M. (ed.) Aerogels Handbook.*
- 408 ADEBAJO, M. O., FROST, R. L., KLOPROGGE, T. J., CARMODY, O. & KOKOT, S.  
409 2003. Porous Materials for Oil Spill Cleanup: A Review of Synthesis and Absorbing  
410 Properties. *Journal of Porous Materials*, 10, 159-170.
- 411 BIGGS, M. J., BUTS, A. & WILLIAMSON, D. 2004. Absolute assessment of adsorption-  
412 based porous solid characterization methods: Comparison methods. *Langmuir*, 20,  
413 7123-7138.
- 414 BRUNAUER, S., EMMETT, P. H. & TELLER, E. 1938. Adsorption of Gases in  
415 Multimolecular Layers. *Journal of the American Chemical Society*, 60, 309-319.
- 416 EL RASSY, H. & PIERRE, A. C. 2005. NMR and IR spectroscopy of silica aerogels with  
417 different hydrophobic characteristics. *Journal of Non-Crystalline Solids*, 351, 1603-  
418 1610.
- 419 FREUNDLICH, H. & HATFIELD, H. 1926. *Colloid and Capillary Chemistry*, London,  
420 Methuen.
- 421 GALARNEAU, A., VILLEMOT, F., RODRIGUEZ, J., FAJULA, F. & COASNE, B. 2014.  
422 Validity of the t-plot Method to Assess Microporosity in Hierarchical  
423 Micro/Mesoporous Materials. *Langmuir*, 30, 13266-13274.

- 424 GREGG, S. J. & SING, K. S. W. 1982. *Adsorption, surface area, and porosity*, London,  
425 Academic Press.
- 426 HRUBESH, L. W., CORONADO, P. R. & SATCHER, J. H. 2001. Solvent removal from  
427 water with hydrophobic aerogels. *Journal of Non-Crystalline Solids*, 285, 328-332.
- 428 JIANG, J.-Q., COOPER, C. & OUKI, S. 2002. Comparison of modified montmorillonite  
429 adsorbents: Part I: preparation, characterization and phenol adsorption. *Chemosphere*,  
430 47, 711-716.
- 431 LIPPENS, B. C. & DE BOER, J. H. 1965. Studies on pore systems in catalysts: V. The t  
432 method. *Journal of Catalysis*, 4, 319-323.
- 433 LOVE, A., HANNA, M. L. & REYNOLDS, J. G. 2003. Engineering surface functional  
434 groups on silica aerogel for enhanced cleanup of organics from produced water.  
435 *Separation Science and Technology*, 40, 311-320.
- 436 OLALEKAN, A. P., DADA, A. O. & ADESINA, O. A. 2014. Review: Silica Aerogel as a  
437 Viable Absorbent for Oil Spill Remediation. *Journal of Encapsulation and*  
438 *Adsorption Sciences*, 4, 122-131.
- 439 PERDIGOTO, M. L. N., MARTINS, R. C., ROCHA, N., QUINA, M. J., GANDO-  
440 FERREIRA, L., PATRÍCIO, R. & DURÃES, L. 2012. Application of hydrophobic  
441 silica based aerogels and xerogels for removal of toxic organic compounds from  
442 aqueous solutions. *Journal of Colloid and Interface Science*, 380, 134-140.
- 443 REYNOLDS, J. G., CORONADO, P. R. & HRUBESH, L. W. 2001. Hydrophobic aerogels  
444 for oil-spill clean up – synthesis and characterization. *Journal of Non-Crystalline*  
445 *Solids*, 292, 127-137.
- 446 SHI, H.-X., CUI, J.-T., SHEN, H.-M. & WU, H.-K. 2014. Preparation of Silica Aerogel and  
447 Its Adsorption Performance to Organic Molecule. *Advances in Materials Science and*  
448 *Engineering*, 2014.
- 449 SIMPSON, E. J., ABUKHADRA, R. K., KOROS, W. J. & SCHECHTER, R. S. 1993.  
450 Sorption Equilibrium Isotherms for Volatile Organics in Aqueous-Solution -  
451 Comparison of Headspace Gas-Chromatography and Online Uv Stirred Cell Results.  
452 *Industrial & Engineering Chemistry Research*, 32, 2269-2276.
- 453 STANDEKER, S., NOVAK, Z. & KNEZ, Z. 2007. Adsorption of toxic organic compounds  
454 from water with hydrophobic silica aerogels. *Journal of Colloid and Interface*  
455 *Science*, 310, 362-368.
- 456 STEPHEN, H. & STEPHEN, T. 1963. *Solubilities of Inorganic and Organic Compounds*,  
457 New York, Macmillan.
- 458 TWUMASI AFRIYIE, E., KARAMI, P., NORBERG, P. & GUDMUNDSSON, K. 2014.  
459 Textural and thermal conductivity properties of a low density mesoporous silica  
460 material. *Energy and Buildings*, 75, 210-215.

- 461 TWUMASI AFRIYIE, E., NORBERG, P., SJÖSTRÖM, C. & FORSLUND, M. 2013.  
462 Preparation and Characterization of Double Metal-Silica Sorbent for Gas Filtration.  
463 *Adsorption*, 19, 49-61.
- 464 WANG, D., MCLAUGHLIN, E., PFEFFER, R. & LIN, J. Y. S. 2011. Adsorption of Organic  
465 Compounds in Vapor, Liquid, and Aqueous Solution Phases on Hydrophobic  
466 Aerogels. *Industrial & Engineering Chemistry Research*, 50, 12177-12185.
- 467 WANG, D., MCLAUGHLIN, E., PFEFFER, R. & LIN, J. Y. S. 2012. Adsorption of oils  
468 from pure liquid and oil-water emulsion on hydrophobic silica aerogels. *Separation  
469 and Purification Technology*, 99, 28-35.
- 470 WANG, J., ZHANG, Y., WEI, Y. & ZHANG, X. 2015. Fast and one-pot synthesis of silica  
471 aerogels via a quasi-solvent-exchange-free ambient pressure drying process.  
472 *Microporous and Mesoporous Materials*, 218, 192-198.
- 473 ZONG, S. K., WEI, W., JIANG, Z. F., YAN, Z. X., ZHU, J. J. & XIE, J. M. 2015.  
474 Characterization and comparison of uniform hydrophilic/hydrophobic transparent  
475 silica aerogel beads: skeleton strength and surface modification. *Rsc Advances*, 5,  
476 55579-55587.
- 477